AIAA JOURNAL
Vol. 33, No. 2, February 1995

Prediction of Supersonic Inlet Unstart Caused by Freestream Disturbances

David W. Mayer* and Gerald C. Paynter†
Boeing Commercial Airplane Group, Seattle, Washington 98124

The objective of this article is to report progress toward the development of an Euler analysis procedure for predicting the unstart tolerance of supersonic inlets. As an aid to understanding boundary condition issues, a one-dimensional, linear-analysis procedure was developed and used to analyze inlet unstart behavior. Using these results as a guide, an Euler analysis procedure was extended through the addition of a new bleed boundary condition, a new compressor face boundary condition, and an engine demand model for the simulation of unsteady inlet flows caused by freestream flow disturbances. Five unstart conditions were identified with the Euler analysis of the axisymmetric inlet for both 20- and 90-deg throat bleed configurations. Results show that both increases and decreases in temperature or velocity will unstart the inlet, whereas only pressure decreases will unstart the inlet. It was also found that 90-deg throat bleed improves the unstart tolerance relative to 20-deg throat bleed for freestream pressure decreases, temperature increases, and changes in velocity.

Nomenclature

A = cross-sectional area
a = speed of sound
C_D = bleed hole discharge coefficient
E = stagnation energy per unit volume
f = $1 + [(\gamma - 1)/2]M^2$
G_1 = $[(\gamma + 1)/2]M_1^2$
J = Jacobian of the coordinate transformation
K_1 = $[2\gamma M_1^2/(\gamma + 1)] - [(\gamma - 1)/(\gamma + 1)]$
K_T = empirical temperature coefficient
M = Mach number
$\dot{m}$ = mass flow rate
$\dot{m}_{\text{lip}}$ = nominal inlet capture flow rate
P = pressure
$\hat{Q}$ = vector of dependent variables
r = radius
T = temperature
t = time
u = x component of velocity vector
V_∞ = freestream velocity
v = y component of velocity vector
x, y = Cartesian coordinates
γ = ratio of specific heats
ϱ = density

Subscripts

bleed = at the bleed system
CF = at the compressor face
c = corrected value
lip = at the inlet lip
nom = nominal condition at the compressor face
r = reference quantity
spill = inlet spillage value
T = stagnation value
throat = flow property in the inlet throat
1 = immediately upstream of the normal shock
$1R$ = nominal shock location
2 = downstream of the normal shock
∞ = freestream quantity

Superscripts

$'$ = after disturbance
$*$ = dimensional quantity

Introduction

SUPERSONIC aircraft encounter a variety of freestream disturbances while in flight. These disturbances in pressure, temperature, and velocity are continuous, random processes that can be described by power spectral density functions with root-mean-squared amplitudes that vary with geographic location and time of year.[1] One source of these disturbances is atmospheric turbulence.[2] When an aircraft encounters atmospheric turbulence, it responds with transient fluctuation in pitch, yaw, and roll angles. These transients, together with the fluctuations in the freestream temperature and pressure, result in disturbances to the stagnation pressure, stagnation temperature, Mach number, and angularity of the inlet flow.

If the propulsion system uses a mixed compression inlet to decelerate and compress the capture flow for the engine, these disturbances can cause expulsion of the normal shock from the inlet, also known as inlet unstart. An unstart results in a loss of propulsive efficiency and can cause an asymmetric pressurization of the wing that would require large control surface forces to maintain aircraft control.

The unstart tolerance of an inlet is defined as the magnitude of the disturbance that can be tolerated by the inlet without an unstart (without use of the inlet control system). Design features of the inlet such as the Mach number distribution through the inlet, the throat Mach number, the normal shock Mach number (i.e., the Mach number immediately upstream of the normal shock), and the design of the bleed system in the vicinity of the throat affect the unstart tolerance. The tolerance can be increased by increasing the rate of throat bleed (bleed between the throat and the normal shock), increasing the throat Mach number, increasing the shock Mach number, and using bleed holes at high angle to the surface. An increase in the tolerance usually reduces the inlet total pressure recovery, increases the total pressure distortion, and increases the bleed drag.

Sanders[3] reported the results of an experimental study of a turbojet engine with a mixed compression inlet operating at Mach 2.5 subjected to both internal and external transient airflow disturbances. He notes that the inlet designer seeks a suitable compromise between the conflicting requirements of high inlet performance and high unstart tolerance.

Presented as Paper 94-0580 at the AIAA 32nd Aerospace Sciences Meeting, Reno, NV, Jan. 10–13, 1994; received Jan. 19, 1994; revision received Sept. 5, 1994; accepted for publication Sept. 5, 1994.

*Senior Specialist Engineer, Propulsion Research Staff. Senior Member AIAA.

†Associate Technical Fellow, Propulsion Research Staff. Associate Fellow AIAA.

In recent years research has been conducted to examine the behavior of supersonic inlets when subjected to unsteady transients.[4–8] Boundary conditions for unsteady Euler and Navier–Stokes (ENS) analyses of inlet flows with either internal or external airflow disturbances are under development.[4,6,7,9] The purpose of this article is to report progress toward the development of one-dimensional and ENS analyses to investigate the effects of freestream pressure, temperature, and velocity disturbances on the flow through a mixed compression inlet and inlet unstart. The analysis was used to investigate how inlet design features affect the unstart tolerance of an axisymmetric mixed compression inlet at a freestream Mach number of 2.35. The salient features of the analysis and the results of the inlet investigation for pressure, temperature, and velocity disturbances are reported in the article.

Approach

The boundary condition problem for ENS simulation of unsteady inlet flows can be divided into two parts. The first part is numerical: how should boundary conditions be imposed on the solution of the finite difference equations to achieve given levels of temporal and spatial accuracy? The second part is the physical modeling represented by the boundary condition: what physical model implemented through a boundary condition adequately represents the flow? For unsteady inlet simulations, the physical modeling problem has proven more difficult than the numerical problem. Early attempts[10] to analyze the dynamics of supersonic inlets neglected the role of boundary-layer bleed in stabilizing the normal shock and modeled the inlet outflow as a convergent-divergent nozzle with a fixed throat area.

Accurate modeling of the bleed and engine face outflow boundaries is key to achieving a successful simulation of an inlet flow subject to either internal or external flow disturbances. Bleed and engine face boundary conditions were developed and reported in Refs. 6 and 7. A quasisteady, one-dimensional analysis of the inlet, similar to that reported by Barry,[2] was used to guide the boundary condition development and to provide insight into how engine face disturbances and bleed affect the motion of the normal shock. An equation reported in Ref. 6 illustrates this insight:

$$\frac{\mathrm{d}\dot{m}_{cCF}}{\dot{m}_{cCF}} + \frac{\mathrm{d}P_{T_2}}{P_{T_2}} + \frac{\mathrm{d}\dot{m}_{\mathrm{bleed}}}{\dot{m}_{\mathrm{bleed}}}\left(\frac{\dot{m}_{\mathrm{bleed}}}{\dot{m}_{CF}}\right) = 0 \qquad (1)$$

Equation (1) shows that if the engine corrected mass flow decreases due to a disturbance at the compressor face, this decrease must be offset by an increase in total pressure downstream of the shock (i.e., forward shock translation) and/or an increase in bleed mass flow. If the disturbance is large enough, Eq. (1) cannot be satisfied with the shock downstream of the inlet throat, and an unstart occurs.

With a freestream disturbance, the unstart problem is more complicated since two unstart mechanisms exist. With a freestream temperature increase or velocity decrease, the Mach number through the supersonic diffuser portion of the inlet is decreased. With the first unstart mechanism, the disturbance decreases the Mach number ahead of the inlet throat to a value less than 1, the inlet throat will no longer pass the capture flow, and the shock is expelled. With the second unstart mechanism, the Mach number in the throat decreases but remains above 1. The disturbance, however, changes the total pressure and temperature at the compressor face, the engine demand changes, and the normal shock moves forward to seek a new match point between the inlet supply flow and the engine demand flow. The forward shock translation increases the rate of throat bleed and increases the total pressure downstream of the normal shock. If the normal shock Mach number becomes less than the throat Mach number, an unstart will occur.

The approach used to investigate the effects of freestream disturbances on the inlet flow is similar to that taken for the engine face disturbance reported in Ref. 7. First, a quasisteady, one-dimensional analysis was developed to provide insight into the effects of a freestream disturbance on the inlet flow. From the one-dimensional analysis, a model was developed for the response of the engine to changes in total pressure and total temperature. Using the bleed boundary condition and an extension to the compressor face boundary condition reported in Ref. 7, freestream perturbations of pressure, temperature, or velocity were imposed and flow solutions were obtained using an Euler simulation of an axisymmetric mixed compression inlet at a freestream Mach number of 2.35. These calculations were run in a time-accurate mode, and the results illustrate the unsteady inlet analysis and the prediction of inlet unstart. The one-dimensional analysis was used as a guide to selecting perturbation magnitudes and as an aid to interpreting the Euler results.

Table 1 Bleed system description

Bleed region	Area, $A_{\mathrm{bleed}}/A_{\mathrm{lip}}$	Hole angle relative to surface, deg	Rows	Row or slot location, x/r_{lip}
Cowl 1	0.00473	20	2	3.1950–3.2349
Cowl 2	0.00462	20	2	3.3951–3.4367
Cowl 3	0.00449	20	2	3.5951–3.6349
Cowl slot	0.0030	——	——	3.7900–3.8300
Cowl 4	0.00760	20	4	3.8816–3.9425
Centerbody 1	0.0070	20	4	3.4167–3.4775
Centerbody 2	0.0055	20	4	3.6190–3.6670
Centerbody 3	0.0070	20	4	3.8175–3.8775

Supersonic Inlet Configuration

A mixed compression translating centerbody inlet (shown in Fig. 1) was used to investigate inlet sensitivity to freestream disturbances. A detailed description of the design is in Ref. 11. The configuration length (measured from the centerbody tip to the compressor face) was 6.3 cowl-lip radii and the centerbody half-angle was 10.3 deg. The flow conditions are for a freestream Mach number of 2.35 at an altitude of 60,000 ft.

The bleed system is described in Table 1. A bleed region consisted of two to four rows of staggered holes with a hole diameter approximately equal to the local boundary-layer displacement thickness just upstream of the bleed band. The holes were spaced between 2.0 and 2.2 hole diameters in a circumferential direction and were angled into the inlet flow.

For the ENS analyses the bleed plenum pressures were set to the freestream static pressure to ensure that all of the bleed regions were choked. The bleed plenum pressure was assumed to be constant for this study so that the flow through a bleed region downstream of the inlet throat remained choked as the normal shock moved forward over the bleed region. The cowl slot was simulated by a porous wall section using discharge coefficient data for 20-deg bleed holes.

One-Dimensional Flow Analysis

The analysis is similar to that reported in Ref. 1. The flow through the inlet is assumed to be steady at both the initial and final flight conditions (the final flight condition is after the instantaneous change in pressure, temperature, or velocity). A change in the freestream causes a change in the Mach number distribution through the throat region and changes the engine flow rate (engine demand). The change in engine demand results in an adjustment in the position of the normal shock until the flow supplied by the inlet is equal to the engine demand.

The analysis requires two steps:

1) The changes in the throat Mach number and the normal shock Mach number (i.e., the Mach number immediately upstream of the normal shock location) are computed as functions of the freestream pressure, temperature, and velocity disturbance magnitudes.

2) The changes in normal shock Mach number, engine airflow, and engine face total pressure are computed as functions of the freestream disturbances, freestream conditions, bleed characteristics, throat conditions, shock conditions, and engine face conditions for a given inlet geometry.

Differential expressions for the change in total pressure across the shock, the change in inlet flow at the compressor face as a function of the shock position, and the linearized change in engine demand form a linear system and can be solved for the change in Mach number at the shock, the change in engine face total pressure, and the change in airflow to the engine. An unstart will occur

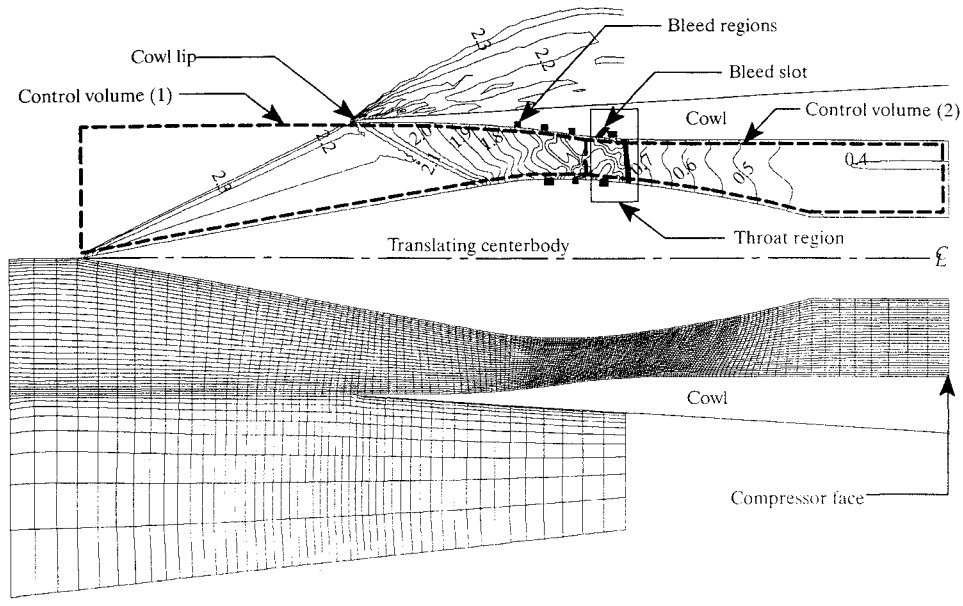

Fig. 1 Axisymmetric mixed compression inlet. Upper half shows Mach contours, lower half shows computational grid.

if the throat Mach number (with the disturbance) is below 1 or if the shock Mach number is less than the throat Mach number. The details of the analysis for the changes in throat and shock Mach number and the linear analysis procedure are summarized in the next section.

Computing Changes in the Throat and Nominal Shock Mach Number

For control volume (1) shown in Fig. 1, a steady-state continuity expression can be written:

$$\dot{m}_{\text{lip}} = \dot{m}_{\text{spill}} + \dot{m}_{\text{bleed}} + \dot{m}_{\text{throat}}$$

Note that $\dot{m}_{\text{lip}}$ is the flow rate into the capture stream tube. Differentiating this expression, assuming that the total pressure in the throat is proportional to the total pressure in the freestream, and assuming that the change in bleed ahead of the throat is negligible with a change in freestream properties, results in

$$\frac{\mathrm{d}M_{\text{throat}}}{M_{\text{throat}}} = f_{\text{throat}}\left\{\left[\frac{\left(1-M_\infty^2\right)}{f_\infty}\right]\frac{\mathrm{d}M_\infty}{M_\infty} - \frac{\mathrm{d}\dot{m}_{\text{spill}}}{\dot{m}_{\text{lip}}}\right\}\Big/\left(f_{\text{throat}} - 3(\gamma-1)M_{\text{throat}}^2\right) \tag{2}$$

where

$$\frac{\mathrm{d}M_\infty}{M_\infty} = \frac{\mathrm{d}V_\infty}{V_\infty} - \frac{1}{2}\frac{\mathrm{d}T_\infty}{T_\infty}$$

Since the Mach number in the throat and in the freestream are assumed to be known, the increase in freestream static pressure, temperature, and velocity are given, and the spillage flow is known (or can be computed) as a function of the change in freestream properties, Eq. (2) can be used to compute the change in throat Mach number that would result from the change in freestream properties.

The spillage flow for an axisymmetric mixed compression inlet is estimated assuming that the conical oblique shock generated by the inlet centerbody is on the lip at the nominal operating condition (zero spillage on-design). If the freestream disturbance increases the freestream Mach number, the spillage is zero because the conical oblique shock from the centerbody will impinge on the cowl inside the lip and all of the flow in the capture stream tube will pass through the inlet. If the freestream disturbance decreases the freestream Mach number, the conical shock from the centerbody moves forward of the lip and some of the flow from the capture stream tube is deflected outside the lip, and the spillage is greater than zero. The spillage for a decrease in freestream Mach number

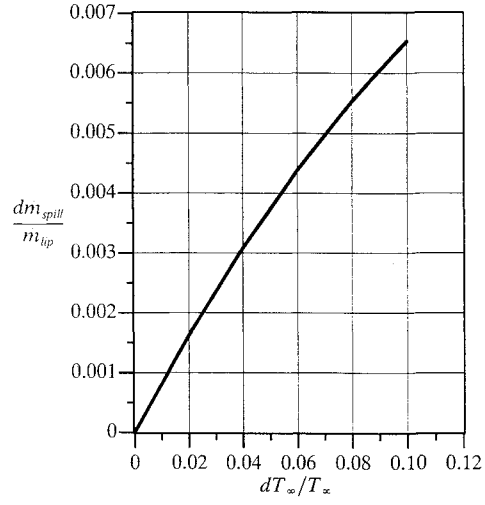

Fig. 2 Estimated spillage due to an increase in freestream static temperature. Axisymmetric inlet with cone half-angle = 10.3 deg, cruise Mach number = 2.35.

is estimated by assuming that the streamline between the conical oblique shock from the centerbody and the lip is a straight line. Reference 12 is used to approximate the streamline slope just downstream of the oblique shock. The estimated spillage for the inlet example as a function of $\mathrm{d}T_\infty/T_\infty$ (a temperature disturbance) is given in Fig. 2.

An expression similar to Eq. (2) is used to compute the change in Mach number at the nominal normal shock location (used in computing the change in Mach number at the shock as the shock location changes to match the change in engine demand).

Shock Loss Function

The expression for the total pressure ratio across a normal shock is

$$P_{T_2}/P_{T_1} = (G_1/f_1)^{\gamma/(\gamma-1)}(1/K_1)^{1/(\gamma-1)}$$

Differentiating this equation leads to the following equation if the total pressure immediately upstream of the shock is assumed to be proportional to the freestream total pressure, and the total pressure

at the compressor face is assumed to be proportional to the total pressure downstream of the shock:

$$\frac{dP_{T_{CF}}}{P_{T_{CF}}} - \gamma M_1^2\left[-\frac{1}{f_1} + \frac{(\gamma+1)}{(\gamma-1)G_1} - \frac{4}{(\gamma-1)(\gamma+1)K_1}\right]\frac{dM_1}{M_1} = \frac{dP_\infty}{P_\infty} + \frac{\gamma M_\infty^2}{2f_\infty}\frac{dM_\infty}{M_\infty} \tag{3}$$

Inlet Flow Function

For control volume (2) shown in Fig. 1, the steady-state continuity equation is

$$\dot{m}_{CF} = \dot{m}_{\text{lip}} - \dot{m}_{\text{spill}} - \dot{m}_{\text{bleed}}$$

Differentiating this equation results in a differential expression for the change in inlet flow rate at the compressor face:

$$\frac{d\dot{m}_{CF}}{\dot{m}_{\text{lip}}} + \left(\frac{C_{D_2}}{C_{D_1}} - 1\right)\frac{M_1}{\Delta M'_{1R}}\frac{\dot{m}_{\text{bleed}_{\text{throat}}}}{\dot{m}_{\text{lip}}}\frac{dM_1}{M_1} = \frac{d\dot{m}_{\text{lip}}}{\dot{m}_{\text{lip}}} - \frac{d\dot{m}_{\text{spill}}}{\dot{m}_{\text{lip}}} + \left(\frac{C_{D_2}}{C_{D_1}} - 1\right)\frac{dM'_{1R}}{\Delta M'_{1R}}\frac{\dot{m}_{\text{bleed}_{\text{throat}}}}{\dot{m}_{\text{lip}}} \tag{4}$$

where

$$\Delta M'_{1R} = M'_{\text{throat}} - M'_{1R}$$

and

$$dM'_{1R} = M'_{1R} - M_1$$

Engine Demand Function

The engine demand function is a differential expression for the change in engine mass flow as a function of the changes in total pressure and temperature at the compressor face. Three engine demand functions have been developed at the Boeing Company, denoted as functions 1, 2, and 3 and by Barry.[2] Implicit in these functions is a model for the response of the engine over the time interval of an unstart (approximately 50 ms) induced by a flow disturbance. Engine demand functions 1, 2, and 3 are thought to represent the current understanding of the engine response and are considered here.

Function 1 was developed from the assumption that the rotational speed of the engine remains constant through a disturbance because of rotational inertia. This assumption is supported by the Sanders[3] experiment. If the rotational speed is constant, then the volumetric flow rate through the engine is approximately constant. The differential expression for the engine demand is

$$\frac{d\dot{m}_{CF}}{\dot{m}_{\text{lip}}} - \frac{\dot{m}_{CF}}{\dot{m}_{\text{lip}}}\frac{dP_{T_{CF}}}{P_{T_{CF}}} = \frac{\dot{m}_{CF}}{\dot{m}_{\text{lip}}}\frac{(M_{CF}^2 - 2)}{2f_\infty}\left[(\gamma-1)M_\infty^2\frac{dV_\infty}{V_\infty} + \frac{dT_\infty}{T_\infty}\right] \tag{5a}$$

Engine demand function 2 was developed from an engine simulation. The differential expression for the engine demand is

$$\frac{d\dot{m}_{CF}}{\dot{m}_{\text{lip}}} - 0.933\frac{\dot{m}_{CF}}{\dot{m}_{\text{lip}}}\frac{dP_{T_{CF}}}{P_{T_{CF}}} = -1.8\frac{\dot{m}_{CF}/\dot{m}_{\text{lip}}}{f_\infty}\left[(\gamma-1)M_\infty^2\frac{dV_\infty}{V_\infty} + \frac{dT_\infty}{T_\infty}\right] \tag{5b}$$

Engine demand function 3 was developed from a linearization of a compressor map (the following equation is an approximation of function 3 valid at 100% design speed):

$$\frac{d\dot{m}_{CF}}{\dot{m}_{\text{lip}}} - \frac{\dot{m}_{CF}}{\dot{m}_{\text{lip}}}\frac{dP_{T_{CF}}}{P_{T_{CF}}} = -\frac{\dot{m}_{CF}/\dot{m}_{\text{lip}}}{f_\infty}\left[(\gamma-1)M_\infty^2\frac{dV_\infty}{V_\infty} + \frac{dT_\infty}{T_\infty}\right] \tag{5c}$$

Solving for M_1, $\dot{m}_{CF}$, and $P_{T_{CF}}$

The inlet flow function, shock loss function, and engine demand function are differential expressions that can be solved for the change in normal shock Mach number, the change in engine face stagnation pressure, and the change in airflow to the engine. That is, Eqs. (3–5) form a linear system of equations that can be solved for the unknowns,

$$\frac{d\dot{m}_{CF}}{\dot{m}_{CF}}, \qquad \frac{dP_{T_{CF}}}{P_{T_{CF}}}, \qquad \frac{dM_1}{M_1}$$

Rewriting Eqs. (3–5) in matrix notation,

$$a_{11}\frac{d\dot{m}_{CF}}{\dot{m}_{\text{lip}}} + a_{12}\frac{dP_{T_{CF}}}{P_{T_{CF}}} + a_{13}\frac{dM_1}{M_1} = b_1$$

$$a_{21}\frac{d\dot{m}_{CF}}{\dot{m}_{\text{lip}}} + a_{22}\frac{dP_{T_{CF}}}{P_{T_{CF}}} + a_{23}\frac{dM_1}{M_1} = b_2$$

$$a_{31}\frac{d\dot{m}_{CF}}{\dot{m}_{\text{lip}}} + a_{32}\frac{dP_{T_{CF}}}{P_{T_{CF}}} + a_{33}\frac{dM_1}{M_1} = b_3$$

Using Cramer's rule to solve for the unknowns,

$$\frac{d\dot{m}_{CF}}{\dot{m}_{\text{lip}}} = \frac{a_{23}b_3 + a_{13}b_2a_{32} - b_1a_{23}a_{32}}{|A|} \tag{6}$$

$$\frac{dP_{T_{CF}}}{P_{T_{CF}}} = \frac{a_{23}b_1 + a_{13}b_3 - b_2a_{13}}{|A|} \tag{7}$$

$$\frac{dM_1}{M_1} = \frac{b_2 + a_{32}b_1 - b_3}{|A|} \tag{8}$$

where

$$|A| = a_{23} + a_{13}a_{32}$$

$$a_{11} = a_{22} = a_{33} = 0$$

$$a_{12} = a_{21} = a_{31} = 1$$

$$a_{13} = -\gamma M_1^2\left[-\frac{1}{f_1} + \frac{(\gamma+1)}{(\gamma-1)G_1} - \frac{4}{(\gamma-1)(\gamma+1)K_1}\right]$$

$$a_{23} = \left(\frac{C_{D_2}}{C_{D_1}} - 1\right)\frac{M_1}{\Delta M'_{1R}}\frac{\dot{m}_{\text{bleed}_{\text{throat}}}}{\dot{m}_{\text{lip}}}$$

with

$$a_{32} = -\frac{\dot{m}_{CF}}{\dot{m}_{\text{lip}}}$$

for engine demand functions 1 and 3, and

$$a_{32} = -0.933\frac{\dot{m}_{CF}}{\dot{m}_{\text{lip}}}$$

for engine demand function 2. The terms for the right-hand side are as follows:

$$b_1 = \frac{dP_\infty}{P_\infty} + \gamma\frac{M_\infty^2}{f_\infty}\frac{dM_\infty}{M_\infty}$$

$$b_2 = \frac{d\dot{m}_{\text{lip}}}{\dot{m}_{\text{lip}}} - \frac{d\dot{m}_{\text{spill}}}{\dot{m}_{\text{lip}}} + \left(\frac{C_{D_2}}{C_{D_1}} - 1\right)\frac{dM'_{1R}}{\Delta M'_{1R}}\frac{\dot{m}_{\text{bleed}_{\text{throat}}}}{\dot{m}_{\text{lip}}}$$

with

$$b_3 = \frac{\dot{m}_{CF}}{\dot{m}_{\text{lip}}}\frac{(M_{CF}^2 - 2)}{2f_\infty}\left[(\gamma-1)M_\infty^2\frac{dV_\infty}{V_\infty} + \frac{dT_\infty}{T_\infty}\right]$$

for engine demand function 1,

$$b_3 = -1.8\frac{\dot{m}_{CF}/\dot{m}_{\text{lip}}}{f_\infty}\left[(\gamma-1)M_\infty^2\frac{dV_\infty}{V_\infty} + \frac{dT_\infty}{T_\infty}\right]$$

for engine demand function 2, and

$$b_3 = -\frac{\dot{m}_{CF}/\dot{m}_{\text{lip}}}{f_\infty}\left[(\gamma-1)M_\infty^2\frac{dV_\infty}{V_\infty} + \frac{dT_\infty}{T_\infty}\right]$$

for engine demand function 3.

One-Dimensional Results

The one-dimensional analysis procedure for freestream disturbances was applied to the axisymmetric mixed compression inlet, Fig. 1, at a nominal freestream Mach number of 2.35. A total inlet bleed rate of 4% and a throat bleed rate equal to 2% of the inlet capture flow were assumed with the throat bleed uniformly distributed between the throat and the normal shock. A throat Mach number of 1.25, a shock Mach number of 1.3 and a compressor face Mach number of 0.42 were also assumed. Only a single throat bleed configuration was considered in the present work. For a throat bleed configuration with 90-deg bleed holes, the throat bleed was assumed to be choked, with the ratio of the discharge coefficient downstream of the normal shock to that upstream of the shock equal to 2.0.

Freestream Static Pressure Perturbation

A 10% increase and a 10% decrease in static pressure were examined for all three engine demand functions. Within the range of static pressure variation investigated, no inlet unstart was predicted.

Freestream Static Temperature Perturbation

For a freestream change in static temperature, predicted throat and shock Mach number results are plotted as a function of the normalized temperature change in Fig. 3. A 4.5% temperature increase was predicted to cause an inlet unstart with engine demand functions 1 and 3, and a 3% increase was predicted to cause an unstart with engine demand function 2. A 12% decrease in freestream static temperature was predicted to cause an unstart with all three engine demand functions. For both an increase and a decrease in temperature, an unstart occurs because the Mach number at the shock required to satisfy the engine demand is less than the throat Mach number.

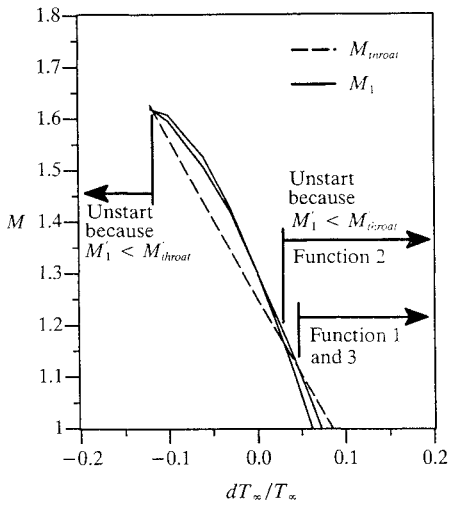

Fig. 3 Predicted change in freestream temperature for inlet unstart. Cruise Mach number = 2.35, cone half-angle = 10.3 deg.

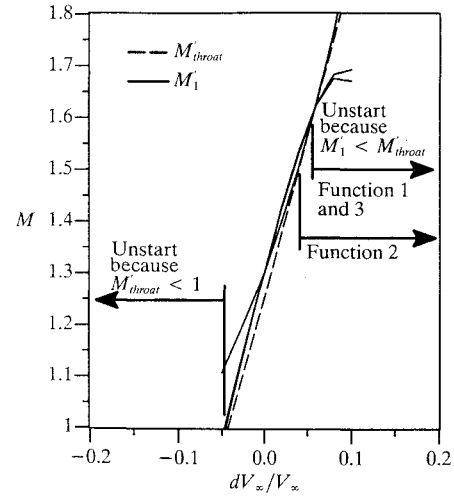

Fig. 4 Predicted change in freestream velocity for inlet unstart. Cruise Mach number = 2.35, cone half-angle = 10.3 deg.

Freestream Velocity Perturbation

Predicted throat and shock Mach number results are plotted as a function of the normalized velocity change in Fig. 4. Note that unstart with a 5% velocity decrease occurs because the throat Mach number falls below 1. A 4% increase in freestream velocity with engine demand function 2 and a 6% increase in freestream velocity with engine demand functions 1 and 3 were predicted to cause an unstart because the throat Mach number was less than the shock Mach number.

ENS Flow Solver

The inlet flowfield calculations were performed with the PARC computer code distributed by the U.S. Air Force.[13] Detailed descriptions of the code are provided in Ref. 13, and only a brief summary of the significant features of the code are presented here. The PARC code is a general purpose flow analysis program based on the ARC code developed at NASA Ames. The code shares many of the features of the original ARC code and has been extensively enhanced for internal flows and for use in an applications-oriented environment.

The basis of the algorithm are the Reynolds-averaged Navier–Stokes equations for a Newtonian fluid that obeys the Fourier heat conduction law. These equations form a system of partial differential equations (i.e., continuity, momentum, and energy equations). The equations are cast in nondimensional conservation law form and then transformed into a general curvilinear coordinate system. The resulting vector of dependent variables is represented by

$$\hat{Q} = \frac{1}{J}\begin{bmatrix} \varrho \\ \varrho u \\ \varrho v \\ E \end{bmatrix}$$

where the nondimensional variables are defined by

$$\varrho \equiv \varrho^*/\varrho_r^*$$

$$u \equiv u^*/a_r^*$$

$$v \equiv v^*/a_r^*$$

$$E \equiv E^*/\left(\varrho_r^* a_r^{*2}\right)$$

and the nondimensional distances, pressures, and temperatures are defined by

$$x \equiv x^*/x_r^*$$

$$P \equiv P^*/\left(\varrho_r^* a_r^{*2}\right) \equiv P^*/(\gamma P_r^*)$$

$$T \equiv T^*/T_r^*$$

Central differences are used to cast the resulting system of equations into finite difference form. The equations are solved using the approximate factorization scheme developed by Beam and Warming, including the diagonalized implicit matrices developed by Pulliam. An alternate flow solver based on the multistage Runge-Kutta method is provided for accurate calculations of time-dependent flows. Implicit residual smoothing may be used to increase the time step size at the expense of reduced temporal accuracy.

Using PARC, complex geometries can be analyzed with relative ease due to the multiblock grid capability and the ability to easily specify boundary conditions on the interior as well as the boundaries of the grid blocks. Inviscid, laminar, and turbulent flows can be simulated for two-dimensional, axisymmetric, or three-dimensional geometries.

Freestream Disturbance Relationships

To facilitate the setting of PARC boundary condition values, relationships between the Mach number, stagnation flow conditions, and the change in static flow conditions have been derived. The next three subsections summarize the derivation of these relationships.

Freestream Mach Number

An expression that relates the freestream Mach number following a disturbance to the nominal freestream Mach number before the disturbance can be derived from the definition of the Mach number

$$\frac{dM}{M} = \frac{dV}{V} - \frac{1}{2}\frac{dT}{T} \tag{9}$$

Equation (9) is used to define the freestream Mach number following a disturbance as a function of the change in freestream temperature and velocity

$$\frac{M'_\infty}{M_\infty} = \frac{\Delta V_\infty}{V_\infty} - \frac{1}{2}\frac{\Delta T_\infty}{T_\infty} + 1 \tag{10}$$

Freestream Stagnation Temperature

Similarly, an expression that relates the freestream stagnation temperature following a disturbance to the nominal freestream stagnation temperature before the disturbance can be derived from the relationship between the stagnation and static temperature. From

$$\frac{T_T}{T} = 1 + \frac{\gamma - 1}{2}M^2$$

it can be shown that

$$\frac{dT_T}{T_T} = \frac{(\gamma - 1)M\,dM}{1 + [(\gamma - 1)/2]M^2} + \frac{dT}{T} \tag{11}$$

Substituting Eq. (9) and collecting terms yields

$$\frac{dT_T}{T_T} = \frac{(\gamma - 1)M^2}{1 + [(\gamma - 1)/2]M^2}\frac{dV}{V} + \frac{1}{\{1 + [(\gamma - 1)/2]M^2\}}\frac{dT}{T} \tag{12}$$

Equation (12) is used to define the freestream stagnation temperature following a disturbance as a function of the change in freestream temperature and velocity

$$\frac{T'_{T_\infty}}{T_{T_\infty}} = \frac{(\gamma - 1)M_\infty^2}{1 + [(\gamma - 1)/2]M_\infty^2}\frac{\Delta V_\infty}{V_\infty} + \frac{1}{\{1 + [(\gamma - 1)/2]M_\infty^2\}}\frac{\Delta T_\infty}{T_\infty} + 1 \tag{13}$$

Freestream Stagnation Pressure

Similarly, an expression that relates the freestream stagnation pressure following a disturbance to the nominal freestream stagnation pressure before the disturbance can be derived from the relationship between the stagnation and static pressure. From

$$\frac{P_T}{P} = \left(1 + \frac{\gamma - 1}{2}M^2\right)^{\frac{\gamma}{\gamma - 1}}$$

it can be shown that

$$\frac{dP_T}{P_T} = \frac{\gamma M\,dM}{1 + [(\gamma - 1)/2]M^2} + \frac{dP}{P} \tag{14}$$

Substituting Eq. (9) and collecting terms yields

$$\frac{dP_T}{P_T} = \frac{\gamma M^2}{1 + [(\gamma - 1)/2]M^2}\left(\frac{dV}{V} - \frac{1}{2}\frac{dT}{T}\right) + \frac{dP}{P} \tag{15}$$

Equation (15) is used to define the freestream stagnation pressure following a disturbance as a function of the change in freestream pressure, temperature, and velocity

$$\frac{P'_{T_\infty}}{P_{T_\infty}} = \frac{\gamma M_\infty^2}{1 + [(\gamma - 1)/2]M_\infty^2}\left(\frac{\Delta V_\infty}{V_\infty} - \frac{1}{2}\frac{\Delta T_\infty}{T_\infty}\right) + \frac{\Delta P_\infty}{P_\infty} + 1 \tag{16}$$

Bleed Boundary Condition

The bleed regions were modeled using the bleed boundary condition developed in Ref. 7. This boundary condition treats each bleed region like a porous wall extending from the front edge of the bleed band to the aft edge. The flow velocity normal to the wall is computed based on the local flow properties, the total bleed hole area, and a discharge coefficient function. The boundary condition is applicable to both steady-state and time-accurate calculations, as well as for inviscid and viscous calculations (i.e., Euler and Navier–Stokes). Since the discharge coefficient of the bleed holes changes, depending on whether the local flow is supersonic or subsonic (i.e., upstream or downstream of the throat normal shock), the bleed boundary condition affects the normal shock motion and the predicted inlet stability.

There is some uncertainty in using this boundary condition for flows with fast transients since the discharge coefficient data are based on empirical data for steady flow. However, the bleed boundary condition is more applicable than the more typical fixed mass-flux bleed boundary condition.

Compressor Face Boundary Condition

Typically, either constant mass flow or constant static pressure are imposed as boundary conditions for subsonic outflow from a fluid dynamic analysis. Based on an engine simulation, it has been shown that at the compressor face, constant volumetric flow is a good approximate description of the effect of the engine on the inlet flow during a short duration disturbance.[8] Constant volumetric flow is also qualitatively consistent with results from the Sanders[3] experiment. These results suggest that it is inappropriate to use constant mass flow or constant static pressure as boundary conditions at the compressor face. Therefore, the compressor face boundary condition developed in Ref. 7 was extended to impose constant volumetric flow at the compressor face boundary.

Starting with Eq. (5a), rewriting in terms of the compressor face stagnation temperature using Eq. (12), and assuming that $T_{T_{CF}} = T_{T_\infty}$ (before a disturbance) yields

$$\frac{d\dot{m}_{CF}}{\dot{m}_{CF}} = \left(\frac{M_{CF}^2}{2} - 1\right)\frac{dT_{T_{CF}}}{T_{T_{CF}}} + \frac{dP_{T_{CF}}}{P_{T_{CF}}}$$

Rewriting in terms of the corrected flow rate and defining $K_T = [(M_{CF}^2 - 1)/2]$ yields

$$\frac{d\dot{m}_{c_{CF}}}{\dot{m}_{c_{CF}}} = K_T\frac{dT_{T_{CF}}}{T_{T_{CF}}}$$

Note that the corrected flow rate is not affected by changes in the stagnation pressure. This equation is then rewritten to yield the corrected flow rate at the compressor face due to a change in the stagnation temperature

$$\frac{\dot{m}_{c_{CF}}\sqrt{T_{T_r}}}{A_{CF}P_{T_r}} = \frac{\gamma M_{\text{nom}}}{\{1 + [(\gamma - 1)/2]M_{\text{nom}}^2\}^{(\gamma+1)/2(\gamma-1)}}\left(K_T\frac{T_{T_{CF}} - T_{T_{\text{nom}}}}{T_{T_{\text{nom}}}} + 1\right)$$

where T_{T_r} and P_{T_r} are reference conditions (typically sea-level static conditions).

There is some uncertainty involved in using this boundary condition for flows with fast transients since the engine demand function is based on a linearized one-dimensional analysis for steady flow immediately before and after the transient. The boundary condition is qualitatively consistent with the available experimental data, however, and should be more appropriate than constant pressure or constant mass flow at the compressor face.

Euler Analysis Results

The effect of instantaneous freestream disturbances has been demonstrated for the axisymmetric mixed compression inlet shown in Fig. 1. The inlet lines were lofted using the CATIA[14] computer-aided design system to define boundaries for the computational fluid dynamics (CFD) grid. The computational grid was generated using

the GRIDGEN2D[15] grid generation program. The axisymmetric calculation was performed using three grid blocks with a total of 5975 grid points. A mesh sensitivity study was not performed; however, based on experience with the code, the grid used for the demonstration calculations is thought to be adequate to define the correct shock jump condition. Grid density does influence the solution accuracy and must be considered when performing design analyses.

Euler calculations were used instead of Navier–Stokes calculations since fewer grid points are necessary and larger time steps are allowed, resulting in less computer time and smaller memory requirements. Euler calculations should provide useful initial design information because the presence of the boundary layer is thought to have only a second-order effect on inlet unstart, provided separation does not exist. The Euler results must be tested against Navier–Stokes and experimental results to determine the validity of using Euler analyses to investigate the effects of freestream disturbances.

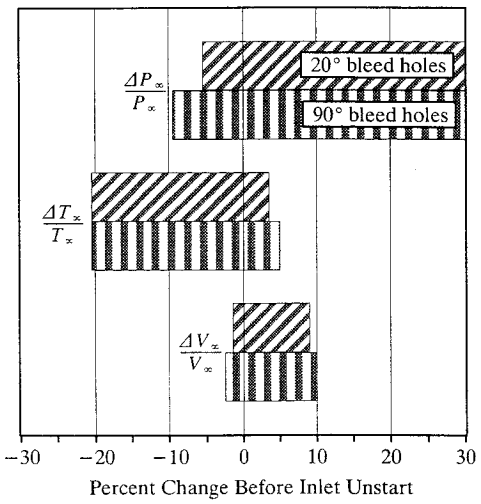

Fig. 5 Instantaneous freestream disturbances that will not cause the inlet to unstart. Cruise conditions: $M_\infty = 2.35$ at 60,000 ft. Note: a limit does not exist for positive pressure disturbances.

Two throat bleed configurations were devised to study the effect of instantaneous freestream disturbances. For the first configuration the bleed hole angle for all bleed bands (including the cowl slot) was assumed to be 20 deg (refer to Table 1). For the second configuration the bleed hole angle for all bleed bands was assumed to be 20 deg except for the cowl slot, cowl 4, and centerbody 3, which were assumed to have 90-deg bleed hole angles. For the second configuration the hole areas for the cowl slot, cowl 4, and centerbody 3 were adjusted so that the bleed rate through these regions matched the values obtained with 20-deg bleed hole angles when the shock was aft of all bleed bands.

Both configurations were run initially for a nominal freestream Mach number of 2.35 at an altitude of 60,000 ft, which corresponds to the following temperature and pressure conditions: $P_\infty = 1.04861$ lbf/in.^{2}, $P_{T_\infty} = 14.1787$ lbf/in.^{2}, $T_\infty = 390$°R, and $T_{T_\infty} = 820.755$°R.

The compressor face Mach number was fixed at 0.4175, and the calculation was run until a steady-state solution was achieved with the throat normal shock just downstream of the throat bleed regions. This steady-state result was used as an initial condition for the freestream disturbance calculations. Mach number contours for this steady-state result are shown in Fig. 1.

Next the compressor face function was used with the nominal Mach number and stagnation temperature from the initial condition calculation (i.e., $M_{\text{nom}} = 0.4175$ and $T_{T_{\text{nom}}} = 820.755$°R). An instantaneous change in the freestream pressure, temperature, or velocity was imposed, and the calculation was run in a time-accurate mode until either the normal shock stabilized in the throat or the inlet unstarted. Using this procedure, the freestream pressure, temperature, or velocity disturbances that would cause the inlet to unstart were found (to the nearest 0.5%). The results from these analyses are summarized in Fig. 5.

Pressure, temperature, and velocity disturbances in the atmosphere are related, as noted in the Introduction. Treating distur-

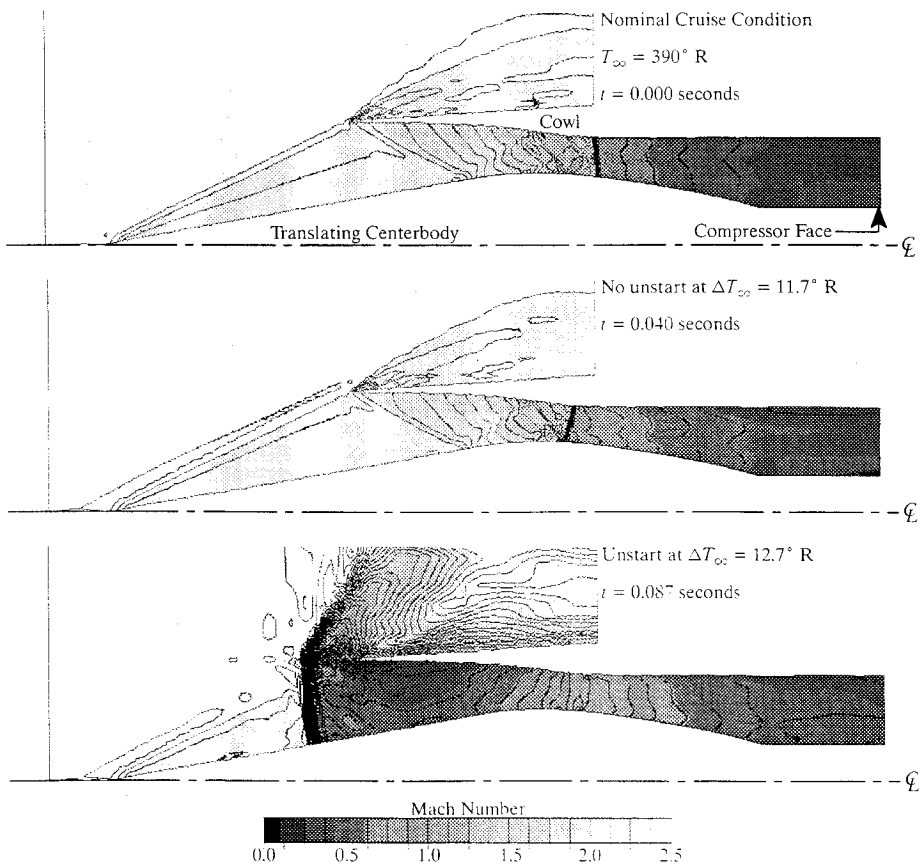

Fig. 6 Freestream temperature disturbance with 20-deg throat bleed.

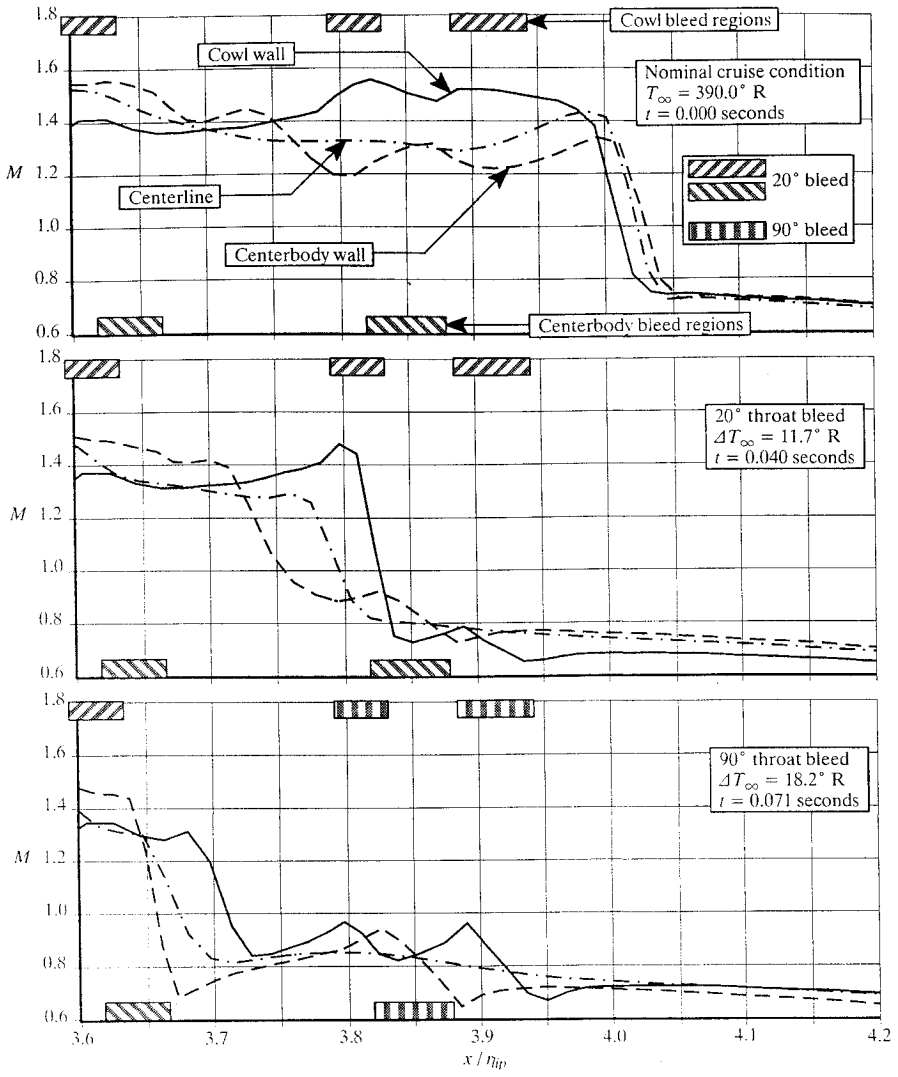

Fig. 7 Throat region Mach profiles along inlet centerline and inlet walls.

bances in these quantities as independent is useful for illustrating the analysis procedure and providing insight but may not be physically meaningful. For example, when an independent change in static pressure is specified at the inflow boundary of the Euler calculation, a change in the freestream velocity (and Mach number) is induced due to the coupling between velocity and pressure that is inherent in the Euler equations.

Changes in freestream temperature are probably the most likely cause of an inlet unstart. Examination of Fig. 5 indicates that an increase in freestream temperature is more likely to cause an inlet unstart than a decrease in freestream temperature. For this reason only the results for instantaneous freestream temperature increases are discussed in detail in the following two subsections. The results due to changes in freestream pressure and velocity are similar.

Freestream Temperature Disturbance with 20-deg Throat Bleed

These calculations were run with a fixed time step size of $5.54 \cdot 10^{-5}$ s and a maximum Courant number of approximately 5. For this case the inlet remained started for freestream temperature increases of up to 11.7°R (i.e., $\Delta T_\infty / T_\infty = 3\%$). For temperature increases of 12.7°R or greater the inlet unstarted as shown in Fig. 6.

The Mach number profiles along the inlet centerline and along both walls are shown in Fig. 7 for $\Delta T_\infty = 11.7$°R. The calculation required 730 time steps to translate the shock forward to the new steady-state condition. The elapsed time for this transient was $4.04 \cdot 10^{-2}$ s.

The residual smoothing option was used to allow calculation at a Courant number of 5. Earlier comparisons with calculations using a smaller Courant number of 0.5 and without residual smoothing did not reveal discernible differences in the steady-state results.[7] With a Courant number of 0.5 the elapsed time for the shock transient was reduced by about 20%, however. Since large Courant numbers result in significantly reduced run times and reduced computer costs, a Courant number of 5 was used for all of the calculations reported in this article. The results are not time accurate due to the size of the Courant number.

Freestream Temperature Disturbance with 90-deg Throat Bleed

For this case the bleed system was nearly the same as for case 1 except that the cowl slot, cowl 4, and centerbody 3 were modeled using 90-deg bleed holes. The flowfield for this configuration was computed to illustrate the effect of the bleed configuration on the inlet tolerance to freestream temperature disturbances. To keep the same initial bleed rate as for case 1, the bleed hole areas for the cowl slot, cowl 4, and centerbody 3 were increased. This increase in bleed hole area was necessary to account for the decrease in the discharge coefficient. The initial condition was the same as for case 1.

The calculation was run with the same time step size and Courant number as case 1. For this case the inlet remained started for freestream temperature increases of up to 18.2°R (i.e., $\Delta T_\infty / T_\infty = 4.7\%$). For temperature increases of 19.2°R or greater, the inlet unstarted as shown in Fig. 8.

The Mach number profiles along the inlet centerline and along both walls are shown in Fig. 7 for $\Delta T_\infty = 18.2$°R. The calculation required 550 time steps to translate the shock forward to the new steady-state condition. The elapsed time for this transient was

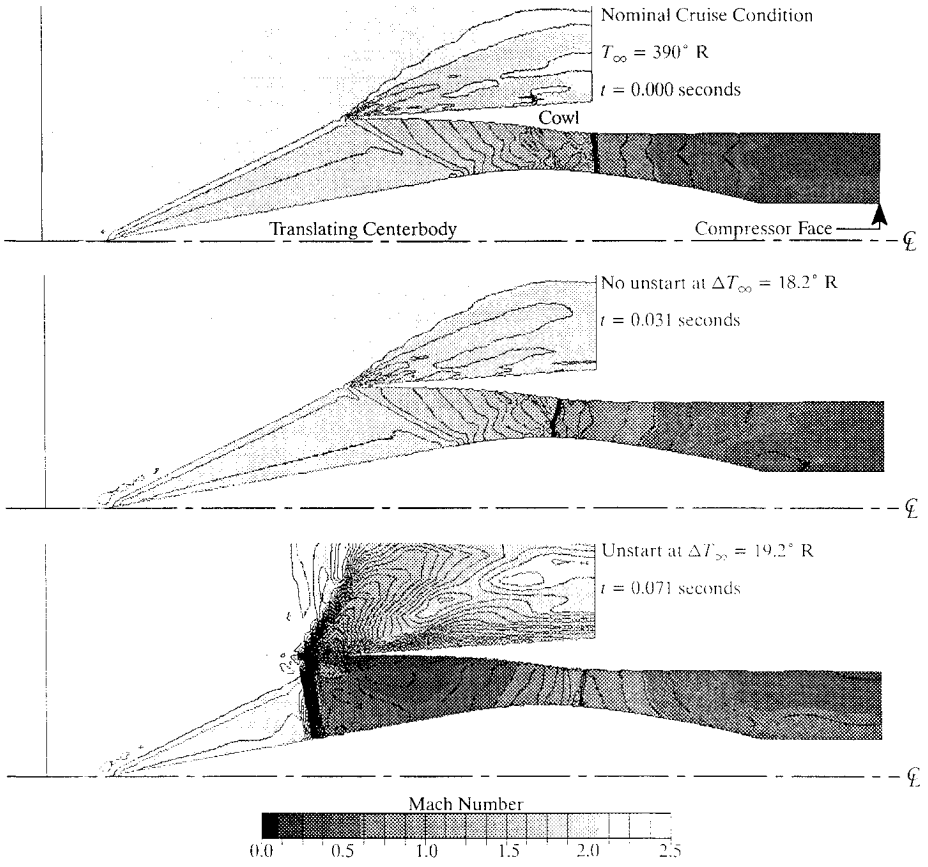

Fig. 8 Freestream temperature disturbance with 90-deg throat bleed.

$3.05 \cdot 10^{-2}$ s (as noted earlier the calculation was run in a time-accurate mode, but the results are not time-accurate due to the size of the maximum Courant number).

Note that a much larger freestream disturbance is tolerated by the inlet with 90-deg throat bleed holes before the inlet unstarts. This indicates that using 90-deg bleed holes leads to an extra margin of stability for the inlet.

Comparison of One-Dimensional and Euler Results

Although qualitative comparisons between the one-dimensional linear analysis and Euler results are possible, direct quantitative comparisons are difficult because different assumptions are made in each analysis.

1) The Euler simulations neglect the boundary-layer blockage (but do include a bleed model that accounts for the change in discharge coefficient as the normal shock moves forward over a bleed band and gives the correct bleed mass flow at a given inlet station). This implies that the PARC predictions of Mach number in the throat and just upstream of the normal shock are slightly too high. Because the throat and shock Mach numbers are specified as input to the one-dimensional analysis, the blockage effect can be accounted for in the simulation.

2) The bleed zones are treated differently in the one-dimensional and the Euler analyses. In the one-dimensional analysis the bleed zone is assumed uniform through the throat region. The Euler analysis includes discrete bleed bands.

3) The flow in the throat is not one dimensional, and it's difficult to determine exactly where the throat is in a PARC simulation (or in a real inlet for that matter). This isn't a problem with PARC, but it is a problem with the one-dimensional analysis. A one-dimensional Mach number could be computed using PARC output data for the mass flow, area, average stagnation pressure, and the average stagnation temperature at an inlet cross section, but it's probably more trouble than it's worth.

4) It is difficult to determine the exact cause of an unstart from the PARC results. An unstart because the Mach number falls below 1 in the throat looks almost exactly like an unstart because the shock Mach number falls below the throat Mach number. The one-dimensional analysis has proven useful in interpreting the PARC results.

5) The one-dimensional analysis allows pressure, velocity, and temperature disturbances to be treated in isolation even though real disturbances will occur simultaneously. Specifying just a freestream pressure perturbation at the inflow boundary with PARC results in an induced velocity change. This velocity change results from the coupling between pressure and velocity in the Euler equations.

Conclusions and Recommendations

A linear-analysis procedure was developed from one-dimensional flow theory to predict the changes in throat Mach number and the normal shock Mach number caused by step changes in freestream static pressure, static temperature, and velocity. The analysis can be used to predict the inlet unstart that will occur if the shock Mach number falls below the throat Mach number or if the throat Mach number falls below 1. For a representative axisymmetric inlet, the analysis was used to predict the magnitude of the freestream static pressure, static temperature, and velocity perturbations required to induce an unstart. Unstart was not predicted with either a 10% increase or decrease in freestream static pressure. Unstart was predicted with both a temperature increase and decrease because the predicted normal shock Mach number was below the throat Mach number. Unstart was predicted with a velocity decrease because the throat Mach number fell below 1, and with a velocity increase because the predicted normal shock Mach number was below the throat Mach number.

An Euler analysis procedure has been developed through the addition of a new bleed boundary condition, a new compressor face boundary condition, and an engine demand model for the simulation of unsteady inlet flows caused by freestream flow disturbances. These procedures are an extension of the analysis for the unsteady flow resulting from a disturbance at the compressor face. The analysis is useful for the prediction of the unstart tolerance of an inlet

flow resulting from a disturbance at the compressor face. The analysis is useful for the prediction of the unstart tolerance of an inlet and the influence of inlet design and flow features on the unstart tolerance.

For each throat bleed configuration five unstart conditions were identified (as shown in Fig. 5). Both increases and decreases in temperature or velocity will unstart the inlet, whereas only pressure decreases will unstart the inlet (a freestream pressure disturbance induced a freestream velocity disturbance). It was also found that 90-deg throat bleed improves the unstart tolerance to velocity disturbances relative to 20-deg throat bleed. The 90-deg throat bleed did not improve the unstart tolerance to decreases in freestream temperature but did improve the unstart tolerance to freestream pressure decreases, temperature increases, and changes in velocity.

The freestream disturbances due to pressure increases, temperature decreases and velocity increases caused the throat normal shock to translate well into the subsonic diffuser portion of the inlet. Since this translation causes the normal shock strength to increase, the normal-shock/boundary-layer interaction can cause the boundary layer to separate when the shock is strong enough. Since Euler calculations do not include viscous effects, the potential for boundary layer separation and inlet unstart due to the separation were not investigated.

In actual practice the inlet will not experience instantaneous freestream disturbances, but it will experience more gradual changes in pressure, temperature, and velocity with time. The results presented, therefore, are qualitative illustrations of the tolerance of the inlet to freestream disturbances. For more gradual disturbances the inlet control system can increase the stability margin if it reacts quickly enough.

Future work should focus on the following tasks:

1) Extend the freestream boundary condition to represent temperature, pressure, and velocity gradients with time (the current PARC boundary condition only allows instantaneous changes to be represented).

2) Validate the solution accuracy.

3) Simulate the inlet flow with a maximum Courant number below 1 to examine the temporal response of the normal shock to freestream and engine disturbances.

4) Extend the bleed boundary condition to account for the temporal response of the bleed plenum pressure to changing bleed flow rates.

5) Validate the use of Euler calculations for unsteady inlet analyses.

6) Run viscous calculations to include throat blockage effects (which affect the throat Mach number distribution, normal shock strength, and normal shock translation), to improve the accuracy of bleed flow rate calculations, and to investigate inlet unstart caused by boundary-layer separation.

7) Define the relationship between freestream pressure, temperature, and velocity disturbances based on an atmospheric model similar to the atmospheric disturbance environment definition provided in Ref. 1.

8) The linear analysis results suggest that the engine demand function has a strong effect on the magnitude of the disturbance predicted to cause an unstart. To date, Euler simulations have been completed with only the constant volumetric engine demand function (function 1). Engine demand functions 2 and 3 should be evaluated with PARC to see if trends similar to those obtained with the linear analysis are predicted.

Acknowledgments

The authors thank their colleagues at the Boeing Company for many valuable discussions and suggestions on the subject of this article. Engine demand function 2 developed by Patricia J. Clark and engine demand function 3 developed by Richard M. Hearsey were important contributions to the successful completion of this article. The constant volumetric engine demand function, function 1, was developed by the second author.

References

[1]Tank, G. W., "Atmospheric Disturbance Environment Definition," NASA CR-195315, Feb. 1994.

[2]Barry, F. W., "Frequency of Supersonic Inlet Unstarts Due to Atmospheric Turbulence," NASA CR-137482, Oct. 1972.

[3]Sanders, B. W., "Dynamic Response of a Mach 2.5 Axisymmetric Inlet and Turbojet Engine with a Poppet-Valve-Controlled Inlet-Stability Bypass System when Subjected to Internal and External Airflow Transients," NASA TP 1531, Jan. 1980.

[4]Chung, J., "Numerical Simulation of a Mixed-Compression Supersonic Inlet Flow," AIAA Paper 94-0583, Jan. 1994.

[5]Benson, R. A., and McRae, D., "Unsteady Transients in a Supersonic Inlet Subject to Freestream Perturbations and Dynamic Attitude Changes," AIAA Paper 94-0581, Jan. 1994.

[6]Paynter, G. C., Mayer, D. W., and Tjonneland, E., "Flow Stability Issues in Supersonic Inlet Flow Analyses," AIAA Paper 93-0290, Jan. 1993.

[7]Mayer, D. W., and Paynter, G. C., "Boundary Conditions for Unsteady Supersonic Inlet Analyses," *Papers from the 11th International Symposium on Air Breathing Engines* (Tokyo, Japan), ISABE 93-7104, International Society for Air Breathing Engines, Vol. 2, 1993, pp. 1062–1070; see also *AIAA Journal*, Vol. 32, No. 6, 1994, pp. 1200–1206.

[8]Decher, R., Mayer, D. W., and Paynter, G. C., "On Supersonic Inlet-Engine Stability," AIAA Paper 94-3371, June 1994.

[9]Chyu, W. J., Howe, G. W., and Shih, T. I.-P., "Bleed Boundary Conditions for Numerically Simulated Mixed-Compression Supersonic Inlet Flow," *Journal of Propulsion and Power*, Vol. 8, No. 4, 1992, pp. 862–868.

[10]Willoh, R. G., "A Mathematical Analysis of Supersonic Inlet Dynamics," NASA TN D-4969, Dec. 1968.

[11]"Advanced Concept Studies for Supersonic Vehicles," NASA CR-145286, Feb. 1978.

[12]Rasmussen, M. L., "On Hypersonic Flow Past an Unyawed Cone," *AIAA Journal*, Vol. 5, No. 8, 1967, pp. 1495–1497.

[13]Cooper, G. K., and Sirbaugh, J. R., "The PARC Code: Theory and Usage," Sverdrup Technology, Inc., AEDC-TR-89-15, Arnold Air Force Base, TN, Dec. 1989.

[14]"CATIA 3D Design, Interactive Functions Reference Manual," International Business Machines Corp., SH50-0091, 1988.

[15]Steinbrenner, J. P., Chawner, J. R., and Fouts, C. L., "The GRIDGEN 3D Multiple Block Grid Generation System," General Dynamics Corp., WRDC-TR-90-3022, Vols. I and II, Fort Worth, TX, July 1990.